Electrocatalysis (2017) 8:189–195
DOI 10.1007/s12678-017-0355-0

ORIGINAL RESEARCH

Synthesis and Characterization of ZrO_2/C as Electrocatalyst for Oxygen Reduction to H_2O_2

Jussara F. Carneiro[1,2] · Leandro C. Trevelin[1] · Alex S. Lima[3] · Gabriel N. Meloni[3] · Mauro Bertotti[3] · Peter Hammer[4] · Rodnei Bertazzoli[2] · Marcos R. V. Lanza[1]

Published online: 4 February 2017
© Springer Science+Business Media New York 2017

Abstract Electrogeneration of hydrogen peroxide (H_2O_2) has potential application in advanced oxidation processes. Amorphous carbon is well known as catalyst for oxygen reduction reaction (ORR) through two-electron pathway. However, modification of the carbon can improve its selectivity for the H_2O_2 electrogeneration. In the present study, we investigated the properties of ZrO_2 nanoparticles supported on carbon black (Printex L6) as electrocatalyst for H_2O_2 production in acidic medium. The catalytic activity of ZrO_2/C for oxygen reduction to H_2O_2 is higher than the catalytic activity of treated carbon black. The highest selectivity of the ZrO_2/C catalyst for H_2O_2 production is attributable to the presence of oxygenated functional groups on its surface and consequently increase of the surface hydrophilicity in comparison with treated carbon black. This surface effect leads to highest H_2O_2 electrogeneration, which is shown as a high current efficiency ($I(H_2O_2)\%$). In fact, increased H_2O_2 yields from 74.5 to 84.2% were observed for the treated carbon black and ZrO_2/C catalysts, respectively, whereas the $I(H_2O_2)\%$ for the unmodified carbon black was 65.3%. Furthermore, the modification of carbon by ZrO_2 nanoparticles shifted the ORR half-wave potential towards ca. 137 mV, indicating lower energy consumption for producing H_2O_2. Thus, the ZrO_2/C nanoparticles are shown to be promising electrocatalysts for environmental applications.

Keywords Zirconium oxide · Oxygen reduction reaction · Hydrogen peroxide · Rotating ring-disc electrode · Scanning electrochemical microscopy

Introduction

Hydrogen peroxide is a green oxidant that is widely used to produce hydroxyl radicals by advanced oxidation process (AOP) for environmental applications. Under acid conditions, H_2O_2 can be produced in situ through oxygen reduction reaction (ORR) using gas diffusion electrodes (GDE) [1]. In general, this reaction is likely to occurs via two paths depending on the electrode material [2, 3], i.e. synthesis of water or H_2O_2 molecules involving four- or two-electron transfer mechanisms, respectively. In alkaline solutions, the ORR through two-electron pathway produces hydroperoxide ion (HO_2^-), the conjugate base of H_2O_2 [4].

Amorphous carbon displays high selectivity towards H_2O_2 production [5]. However, modification of the carbon can improve its catalytic activity for ORR [6–8]. Zirconium oxide is an acidic oxide that contains Brønsted surface sites [9] which can provide higher hydrophilicity to the nanostructured carbon electrode and, consequently, increase the selectivity for

Electronic supplementary material The online version of this article (doi:10.1007/s12678-017-0355-0) contains supplementary material, which is available to authorized users.

✉ Marcos R. V. Lanza
marcoslanza@iqsc.usp.br

Jussara F. Carneiro
jussarafcarneiro@iqsc.usp.br

[1] Instituto de Química de São Carlos, Universidade de São Paulo, Avenida Trabalhador São Carlense 400, São Carlos, SP 13566-590, Brazil

[2] Faculdade de Engenharia Mecânica, Universidade Estadual de Campinas, Rua Mendeleyev 200, Campinas, SP 13083-860, Brazil

[3] Departamento de Química Fundamental, Instituto de Química, Universidade de São Paulo, Avenida Prof. Lineu Prestes 748, Butantã, São Paulo, SP 05508-900, Brazil

[4] Instituto de Química, Universidade Estadual Paulista, Rua Professor Franscisco Degni 55, Araraquara, SP 14800-060, Brazil

the H_2O_2 electrogeneration [10]. Furthermore, since ZrO_2 is a stable oxide in acidic media, it can be used in Fenton process.

As reported by Mittermeier et al. [11], the ORR activity of ZrO_2-based carbon-supported nanoparticles is not conclusively described in literature. The catalytic activity of this oxide depends on the morphological and structural proprieties consequently on the synthesis method. Mittermeier et al. [11] studied the interplay of Zr, N and C species vs. the applied heat-treatment procedure. ZrOPc (precursor containing Zr and N) supported on Ketjenblack (ZrOPc/KB) and KB substrate exhibit high H_2O_2 yields in alkaline electrolyte. However, in acid solution, the ORR activity is much smaller for the ZrOPc/KB catalyst and negligible for the KB reference material.

Ota et al. [12] investigated Zr-based materials as cathode of a direct methanol fuel cell (DMFC) without platinum in order to improve the stability of non-noble-metal ORR electrocatalysts in acidic medium. According to the authors, the sub-oxide of zirconia, ZrO_{2-x}, shows good activity for the ORR through four-electron pathway. Thus, ZrO_{2-x} could be a good cathode material for DMFCs.

Iwazaki et al. [13] compared the catalytic activity of carbonized silk fibroin with those of activated carbons. The activation of the carbon substrate promotes the ORR through 3.5 electrons transfer. However, the addition of ZrO_2 at 20 wt% improves the oxygen reduction to H_2O through 3.9 electrons transfer.

As reported previously [14, 15], low amount of metal oxide tends to promote the oxygen reduction through two-electron pathway whereas higher amount tends to promote the ORR through four-electron pathway. Therefore, in the present study, we investigated the properties of ZrO_2 nanoparticles (5.0 wt%) supported on carbon black as an electrocatalyst for producing H_2O_2 in acid medium.

Experimental

Preparation of ZrO_2/C Nanoparticles

ZrO_2 supported onto carbon black (Printex L6 carbon, Evonik Co.) was synthesized by thermal decomposition of a polymeric precursor solution [16] containing zirconium carbonate [$(ZrO_2)_2.CO_2$, Alfa Aesar] as a salt precursor. In a typical experiment, $(ZrO_2)_2.CO_2$ was added to a citric acid:ethylene glycol suspension at a molar ratio of 1:10:40, respectively. The mixture was continuously stirred by a magnetic stirrer for 60 min at 60 °C. Carbon black was then added slowly to this mixture. The resulting dispersion was heated in air at a rate of 3 °C min^{-1} and treated at 500 °C for 30 min. The final Zr concentration in the catalyst was 5.0% (*w*/*w*). The carbon matrix was also treated following the same procedure but without adding the $(ZrO_2)_2.CO_2$ precursor at the first step.

Physical-Chemical Characterizations

Morphological and chemical characterizations were performed by X-ray diffraction (XRD), transmission electron microscopy (TEM), X-ray photoelectron spectroscopy (XPS) and contact angle (θ) measurements.

XRD was conducted on a Rigaku diffractometer operating with CuK_α radiation source (λ = 1.54056 Å) at 40 kV and 80 mA. Crystalline phases were identified by comparison with standard XRD patterns available at International Center for Diffraction Data (Joint Committee on Powder Diffraction Standards—JCPDS). TEM images were registered with a JEOL JEM-2100 transmission electron microscope running at 200 kV. XPS spectra were measured at a pressure lower than 10^{-7} Pa using a UNI-SPECS UHV spectrometer equipped with an MgK_α X-ray source ($h\nu$ = 1253.6 eV) and analyser pass energy set at 10 eV. The inelastic background of C (1s), O (1s) and Zr (3d) electron core-level spectra was subtracted using Shirley's method. The spectra were fitted without constraints using multiple Voigt profiles. Contact angle (θ) was determined on an angle meter (Attension Theta) by dropping a water droplet (3 μL) onto the catalyst surface.

Electrochemical Characterization

Electrochemical measurements were initially performed on a potentiostat/galvanostat Autolab PGSTAT 128 N (Metrohm) equipped with a rotating ring-disc electrode system (Pine Instruments). The working electrode was prepared by dispersing 1 mg of catalyst into 1 mL of water under sonication for 30 min, as described by Paulus et al. [17]. Then, an aliquot suspension of 20 μL was carefully dropped onto the glassy carbon electrode disc of the RRDE (5.6 mm diameter). The resulting microlayer was slowly dried in air. All electrochemical studies were carried out on a conventional electrochemical cell using Ag/AgCl (3.0 mol L^{-1} KCl) as a reference electrode, a Pt plate as a counter electrode and 0.1 mol L^{-1} K_2SO_4 (pH 2, adjusted by H_2SO_4) as the electrolyte solution.

Cyclic voltammetric (CV) curves were recorded in N_2-saturated solution at a scan rate of 10 mV s^{-1}. Linear sweep voltammetric (LSV) curves were recorded in N_2 and O_2-saturated solution. The disc electrode potential was scanned at a rate of 5 mV s^{-1} while the ring electrode potential was kept at constant value of +1.0 V in order to measure the anodic current equivalent to the H_2O_2 molecules produced at the disc electrode surface. RRDE measurements were performed at rotation speeds ranging from 100 to 2500 rpm. Carbon black and commercial Pt/C (20 wt.% on Vulcan XC-72 carbon- E-TEK) were used as reference materials for two- and four-electron pathways, respectively. All LSVs presented in this work were corrected by subtracting the current background, which was registered in N_2-saturated solution.

SECM Measurements

SECM experiments were conducted on a Sensolytics SECM workstation (Sensolytics) instrument with High-Res option. The equipment was coupled to an Autolab PGSTAT 128N (Metrohm) bipotentiostat. The SECM tip was a 20-μm-width Pt disc-shaped microelectrode characterized by an insulating glass sheath radius (rg) to active Pt electrode radius (a) ratio, known as RG (RG = rg/a), of approximately 10. The microelectrode was fabricated using a P-97 Flaming/Brown Micropipette Puller (Sutter Instrument Company).

SG/TG experiments were carried out with a tip to substrate distance of 60 μm. This relatively large distance enabled the substrate surface to be scanned by the tip at a constant height without the risk of tip crashing. This experimental condition also allowed high data acquisition efficiency due to the intrinsic characteristics of the SG/TC SECM setup (high mass transport at the microelectrode and confinement of material produced onto the substrate). The tip was positioned using H^+ as a redox mediator [18]. In order to increase the tip response and stability, the microelectrode surface was modified by platinum deposition in accordance with the procedure described by Schuhmann et al. [19].

Results and Discussion

XRD, TEM and XPS Analyses

Powder XRD patterns of the treated carbon black and ZrO_2/C catalysts are presented in Fig. 1. The peaks at 30.1°, 34.9°, 50.2° and 59.7° of 2θ shown in the XRD pattern of ZrO_2/C (Fig. 1A) correspond to the (111), (200), (220) and (311) planes of ZrO_2 cubic phase (JCPDS#89-9060) (Fig. 1C). The broad reflections seen at approximately 24.7° and 43.5° of 2θ are ascribed to the amorphous carbon matrix phase (Fig. 1B) [5].

Figure 2A shows a representative TEM image of the ZrO_2/C catalyst. It can be observed that the ZrO_2 nanoparticles are uniformly distributed within the carbon support. The average size obtained from 100 randomly selected nanoparticles was 2.6 ± 0.3 nm (Fig. 2B). The selected area electron diffraction (SAED) pattern reveals a typical polycrystalline profile (Fig. 2C). The interplanar distances of 2.96, 2.57 and 1.81 Å correspond to the (111), (200) and (220) planes, respectively, of the ZrO_2 phase (JCPDS#89-9060). These results are in close agreement with the XRD data.

The local bonding structure of the ZrO_2/C catalyst was investigated through analysis of the C (1s), O (1s) and Zr (3d) core-level XPS spectra. The fitted high-resolution C (1s) XPS spectrum of ZrO_2/C (Fig. 3a) can be deconvoluted into five sub-peaks, which corresponded to sp^2 C–C bonds at 284.4 eV, C–H bonds at 285.5 eV, epoxy C–O bonds at 286.5 eV, carbonyl C=O bonds at 287.5 eV and carboxyl O–C=O bonds at 289.4 eV [20].

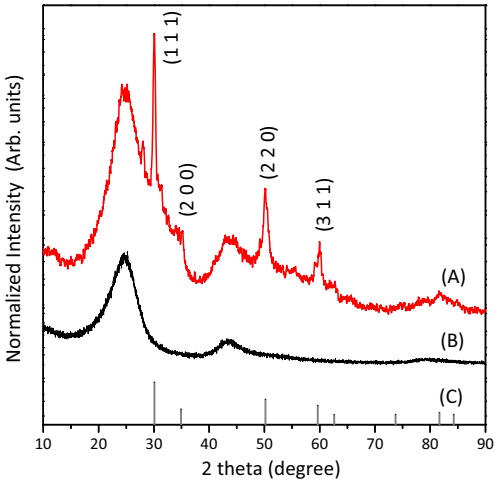

Fig. 1 Powder XRD patterns of (*A*) ZrO_2/C catalyst (*B*), treated carbon black and (*C*) JCPDS standard of ZrO_2 phase (#89-9060)

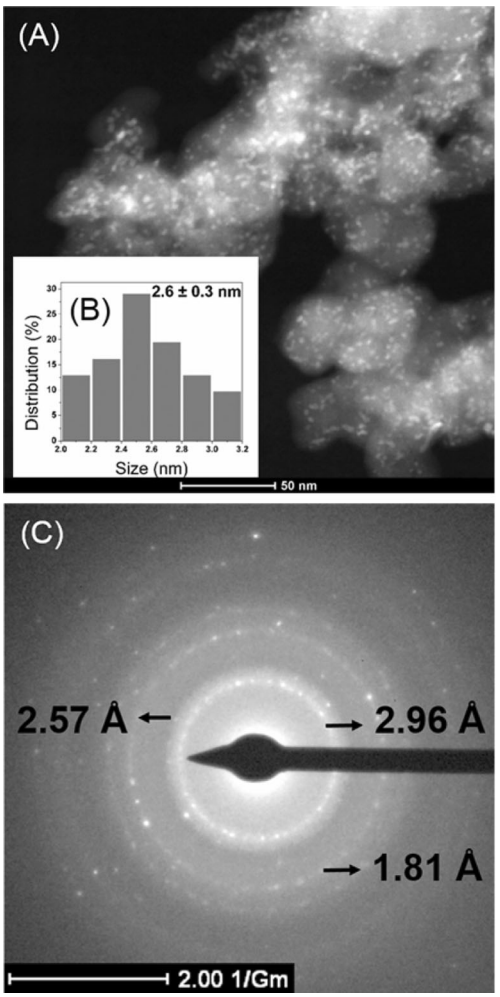

Fig. 2 (*A*) TEM image of ZrO_2 nanoparticles supported on carbon black. (*B*) Particle size distribution of ZrO_2 nanoparticles. (*C*) SAED pattern of ZrO_2/C catalyst

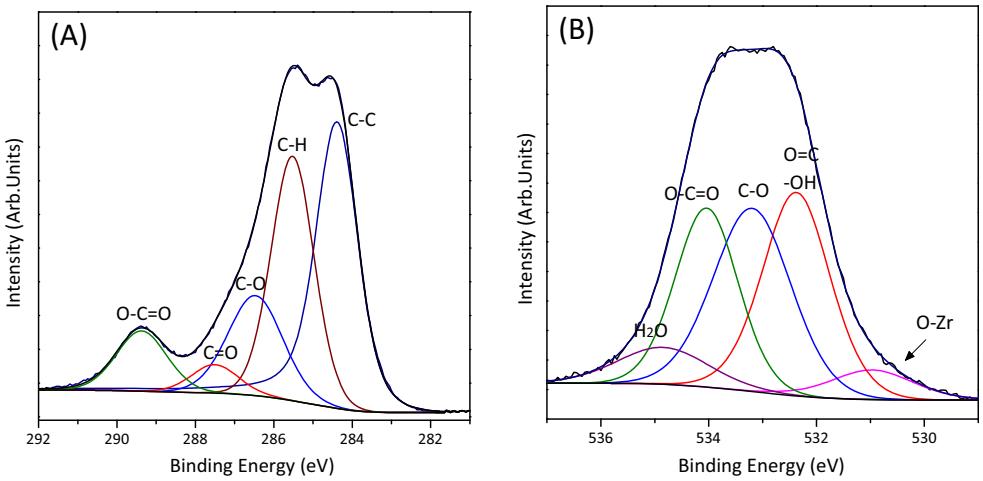

Fig. 3 High-resolution XPS spectra **a** C 1s and **b** O 1s of ZrO_2/C catalyst

The presence of oxygenated functional groups on the ZrO_2/C surface promotes electron transfer, thereby enhancing the ZrO_2/C catalytic activity on oxygen reduction [21, 22].

The O (1s) XPS spectrum of ZrO_2/C (Fig. 3b) can be attributed to carbonyl groups (C=O) at 532.3 eV, alcohols groups (C–O) at 533.1 eV and carboxyl groups (O–C=O) at 533.8 eV [20]. This confirms the presence of the oxygenated groups previously identified in the C (1s) spectrum. A small peak at 530.8 eV is related to O–Zr bonds [20] of ZrO_2 nanoparticles embedded within the carbon substrate. Another possible chemical bond at ca. 532.8 eV can be attributed to Zr–OH that overlaps with the carbonyl groups peak. The weak high-energy component at 535.0 eV corresponds to water molecules adsorbed onto the ZrO_2/C nanoparticle surface.

Figure 4 shows the Zr (3d) spin-orbit XPS spectrum ($3d_{5/2}$ and $3d_{3/2}$) of the ZrO_2/C catalyst. The Zr $3d_{5/2}$ peak position at 185.5 eV corresponds to ZrO_2 phase, even though it is slightly shifted towards higher binding energies. This may suggest the presence of zirconium hydroxide on the catalyst surface [20].

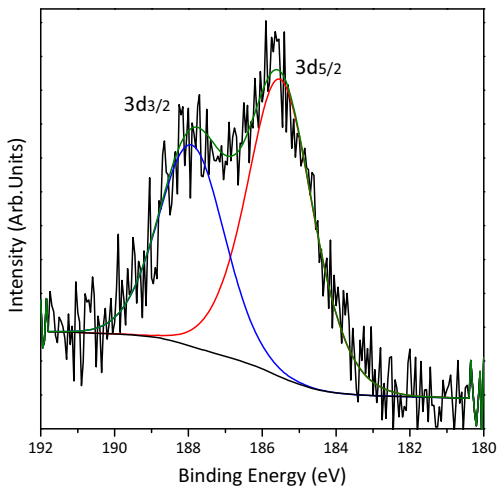

Fig. 4 Deconvoluted Zr 3d spectrum of ZrO_2/C catalyst

CV and LSV Analysis

Electrochemical properties of treated carbon black and ZrO_2/C catalysts were first examined by CV experiments recorded between +0.6 and −0.6 V at a scan rate of 10 mV s^{-1}. Figure 5 displays the cyclic voltammograms recorded in nitrogen- (dash) and oxygen-saturated (solid) 0.1 mol L^{-1} K_2SO_4 solution at pH 2. In N_2-saturated solution, the voltammetric behaviour of treated carbon black was characterized by absence of peaks throughout the applied potential range. On the other hand, the ZrO_2/C catalyst showed a broad peak from +0.4 to 0.0 V, which may be attributed to the presence of oxygenated functional groups on its surface [23]. In O_2-saturated solution, the treated carbon black showed one cathodic peak at ca. −0.39 V which may be ascribed to oxygen reduction activity on its surface. The ORR peak potential of the ZrO_2/C

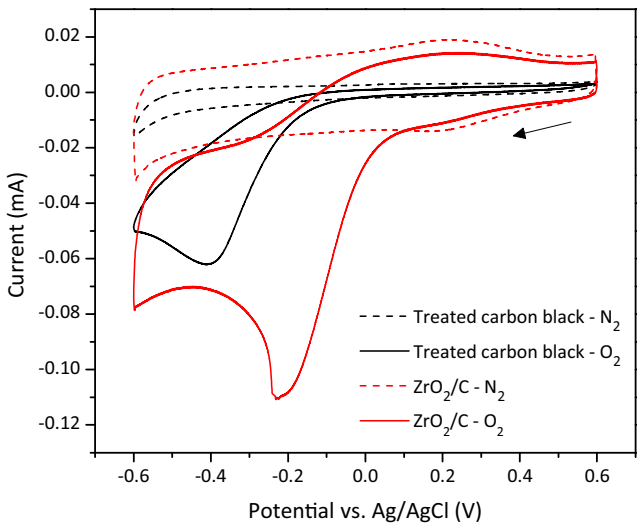

Fig. 5 Cyclic voltammetric profiles of treated carbon black and ZrO_2/C catalysts recorded in nitrogen- (*dash*) and oxygen- (*solid*) saturated 0.1 mol L^{-1} K_2SO_4 solution (pH = 2) at 10 mV s^{-1}

catalyst, at ca. –0.20 V, was less negative than that of carbon black, suggesting higher electrocatalytic activity to oxygen reduction at lower overpotential.

In order to investigate the catalytic effect of ZrO_2/C on the ORR, the electrochemical behaviour of electrodes widely used for oxygen reduction through two-electron (carbon black—Printex L6) and four-electron (Pt/C—E-TEK, 20% wt.) transfer was studied using rotating ring-disc electrode. In this system, the current values recorded at the disc electrode (I_d) refer to ORR while the current determined at the ring electrode (I_r) refer to H_2O_2 electrogeneration from ORR.

Fig. S1A-B shows the linear sweep voltammograms obtained in 0.1 mol L^{-1} K_2SO_4 solution (pH 2) at different rotation speeds for the treated carbon black and Pt/C. The polarization curves exhibited a typical profile in which the reduction current densities increases with increasing rotation speed due to shortened diffusion lengths at high speeds [24]. Furthermore, the disc currents are successively controlled by kinetic (charge transfer), mixed and diffusion control (O_2 mass transport) [25].

As shown in Fig. S1A, the ring currents for treated carbon black increased gradually with increasing negative potential, indicating reduction of oxygen into H_2O_2 [26]. It is known that ORR on Pt/C electrode proceeds through a four-electron pathway [17], and this was confirmed by the RRDE measurements obtained in the present study (Fig. S1B). LSVs recorded within the potential range from +1.0 to −0.2 V showed that the ring currents are negligible, thus confirming reduction of oxygen to H_2O.

Figure 6a displays LSVs of carbon black, treated carbon black and ZrO_2/C catalysts recorded in 0.1 mol L^{-1} K_2SO_4 solution (pH 2) at rotation rate of 900 rpm. The treatment of carbon enhanced its selectivity for H_2O_2 electrogeneration. As reported previously by our group [22], the high ORR activity of treated carbon is ascribed to the increase in oxygen-containing functional groups onto the carbon surface by polymeric precursor method. The polarization curve of the ZrO_2/C catalyst showed higher ring currents than those obtained with the treated carbon black, indicating larger H_2O_2 electrogeneration. Furthermore, the modification of carbon by ZrO_2 nanoparticles deposition led to a positive shift of the half-wave potential of ca. 137 mV, which is supported by the CVs profile in O_2-saturated solution (Fig. 5). This shift in ORR potential enables oxygen reduction with lower energy consumption.

Koutecky-Levich plots for treated carbon black, Pt/C and ZrO_2/C catalysts are shown in Fig. 6b. The linearity and parallelism of the fitting lines for treated carbon and ZrO_2/C indicated similar electron transfer number for oxygen reduction and first-order kinetics reaction [27]. Extrapolation of the Koutecky-Levich plots revealed non-zero intercepts, suggesting that the oxygen reduction occurs under mixed control [25].

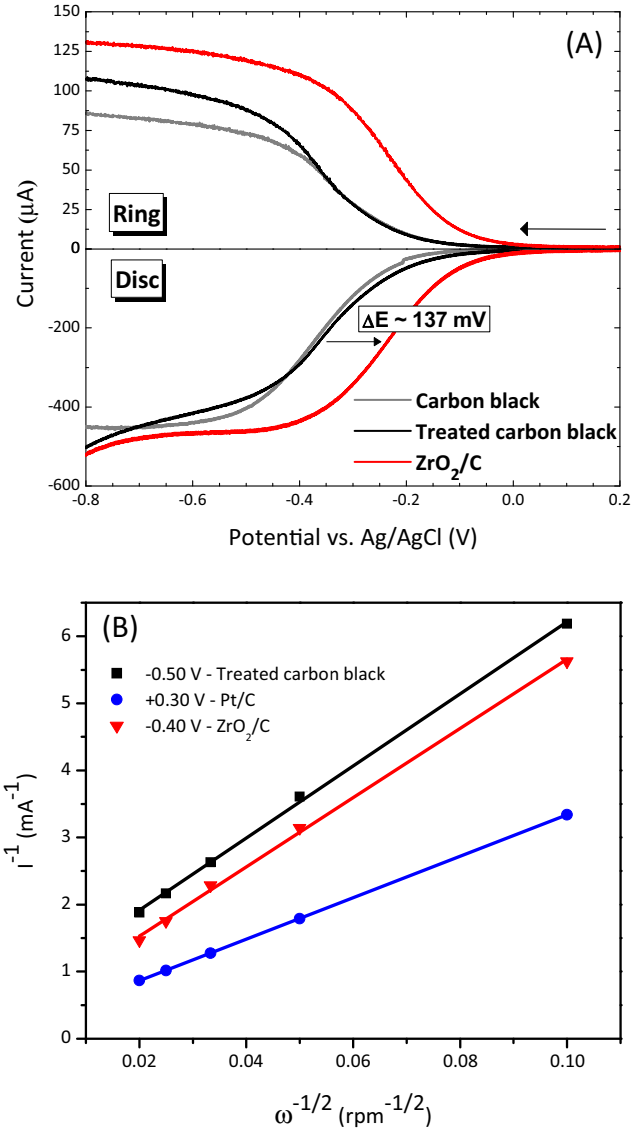

Fig. 6 **a** Steady-state polarization curves for ORR evaluation using RRDE for carbon black, treated carbon black and ZrO_2/C. The curves were recorded in 0.1 mol L^{-1} K_2SO_4 solution (pH 2) with scan rate of 5 mV s^{-1} at 900 rpm. **b** Koutecky-Levich plots of treated carbon black, Pt/C and ZrO_2/C catalysts. The LSVs data of carbon black and treated carbon black are Copyright© by Carneiro et al. [22]

Quantitative analysis of hydrogen peroxide production ($I(H_2O_2)\%$) and electron transfer number (n_t) were determined by the following equations [17]:

$$I(H_2O_2)\% = \frac{200 \cdot I_r/N}{I_d + I_r/N} \quad (1)$$

$$n_t = \frac{4 \cdot I_d}{I_d + I_r/N} \quad (2)$$

where N is the current collection efficiency of the Pt ring ($N = 0.37$) polarized at +1.0 V to the H_2O_2 detection.

The H_2O_2 electrogeneration on the treated carbon black and ZrO_2/C catalysts were 74.5 and 84.2%, respectively.

The electron transfer number of these catalysts was similar, i.e. 2.3 for ZrO_2/C versus 2.5 for treated carbon black. This value is consistent with results obtained from Koutecky-Levich plots based on RRDE voltammograms. For the unmodified carbon black, the $I(H_2O_2)$% was 65.3%, while the n_t was 2.7. Additionally, the values obtained using Pt/C confirmed that this catalyst promotes ORR through the four-electron pathway, i.e. displaying a n_t value of 3.9.

SECM Analysis

In order to examine the substrate potential influence on the ORR and to confirm the ZrO_2/C selectivity for H_2O_2 production, SECM SG/TC experiments were carried out in 0.1 mol L^{-1} K_2SO_4 solution (pH 2). With the tip positioned 60 μm above the substrate and held the potential at +1.0 V to oxidize any H_2O_2 molecule produced, the substrate potential was swept between +0.2 to −0.8 V in a LSV experiment, while both tip and substrate currents were recorded. Treated carbon black and ZrO_2/C were used as substrates for the ORR process.

According to the SG/TC experiments (Fig. 7), the electrocatalytic activities of both catalysts towards the ORR were almost the same ($I_{subst.}$), although the ZrO_2/C showed a slightly lower overpotential. Regarding the selectivity for H_2O_2 production, the ZrO_2/C-modified substrate presented a higher current at the tip (I_{tip}) in the region of mixed control, i.e. from ca. –0.10 to ca. –0.55 V, confirming the higher selectivity of ZrO_2/C towards ORR involving two-electron transfer. The increase in substrate reduction current values at potentials more negative than −0.6 V refers to hydrogen evolution reaction in the acidic electrolyte solution.

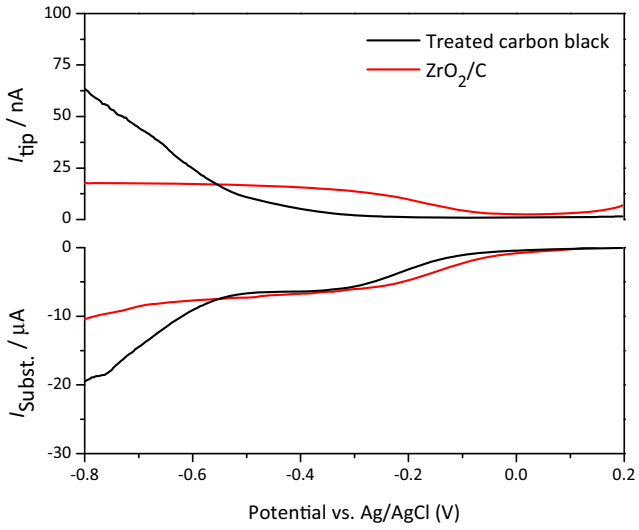

Fig. 7 SG/TC voltammograms of treated carbon black and ZrO_2/C. Curves were recorded in 0.1 mol L^{-1} K_2SO_4 solution (pH 2) with tip to substrate distance of 60 μm in the potential range of +0.2–0.8 V. The tip potential was kept constant at +1.0 V

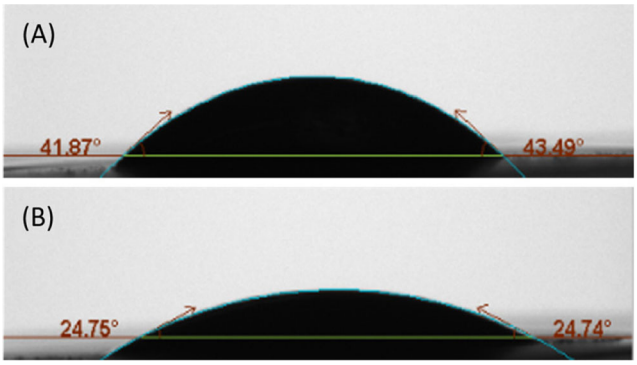

Fig. 8 Contact angle images of ultra-pure water droplet onto **a** treated carbon black and **b** ZrO_2/C surfaces

Contact Angle

Finally, the wettability of the treated carbon black and ZrO_2/C surfaces was examined by the water droplet contact angle, which is geometrically defined as the angle formed by a liquid at the solid-liquid-gas interface (Fig. 8.)

As shown in Fig. 8, the contact angle decreased from ca. 42° to 24° after modifying the carbon with ZrO_2 nanoparticles. Thus, the presence of ZrO_2 on the carbon surface increases the carbon wettability and consequently the hydrophilicity of the catalyst surface. Moreover, the improved hydrophilic property can be attributed to the presence of oxygenated functional groups onto the ZrO_2/C surface (Fig. 3) [28], which are present in an amount higher than that of treated carbon, as earlier reported by our group [22]. This effect leads to the high selectivity of the ZrO_2/C catalyst for H_2O_2 electrogeneration.

Conclusions

ZrO_2 nanoparticles deposited on carbon black were prepared by a polymeric precursor method. The catalytic activity of ZrO_2/C for oxygen reduction to H_2O_2 is higher than the catalytic activity of treated carbon black. The highest selectivity of the ZrO_2/C catalyst for H_2O_2 production is attributable to the increase in the surface hydrophilicity in comparison with treated carbon black. Furthermore, the presence of ZrO_2 on carbon shifts the ORR overpotential towards ca. 137 mV, indicating lower energy consumption for producing H_2O_2. Therefore, ZrO_2/C catalysts can be efficiently used for in situ H_2O_2 production in gas diffusion electrode, thus in advanced oxidation processes.

Acknowledgements The authors acknowledge the financial support of Conselho Nacional de Desenvolvimento Científico e Tecnológico (CNPq—grants 163689/2015-6, 160507/2011-1 and 470079/2013-4), Fundação de Amparo à Pesquisa do Estado de São Paulo (FAPESP—grants 2011/14314-1, 2016/01937-4) and Coordenação de Aperfeiçoamento de Pessoal de Nível Superior (CAPES).

References

1. A. Da Pozzo, L. Di Palma, C. Merli, E. Petrucci, An experimental comparison of a graphite electrode and a gas diffusion electrode for the cathodic production of hydrogen peroxide. J. Appl. Electrochem. **35**, 413–419 (2005). doi:10.1007/s10800-005-0800-2
2. E. Yeager, Electrocatalysts for O2 reduction. Electrochim. Acta **29**, 1527–1537 (1984). doi:10.1016/0013-4686(84)85006-9
3. E. Yeager, Dioxygen electrocatalysis: mechanisms in relation to catalyst structure. J. Mol. Catal. **38**, 5–25 (1986). doi:10.1016/0304-5102(86)87045-6
4. F.C. Moreira, R.A.R. Boaventura, E. Brillas, V.J.P. Vilar, Electrochemical advanced oxidation processes: a review on their application to synthetic and real wastewaters. Appl. Catal. B Environ. **202**, 217–261 (2017). doi:10.1016/j.apcatb.2016.08.037
5. M.H.M.T. Assumpção, R.F.B. De Souza, D.C. Rascio, J.C.M. Silva, M.L. Calegaro, I. Gaubeur, et al., A comparative study of the electrogeneration of hydrogen peroxide using Vulcan and Printex carbon supports. Carbon N. Y. **49**, 1842–2851 (2011)
6. J.C. Forti, R.S. Rocha, M.R.V. Lanza, R. Bertazzoli, Electrochemical synthesis of hydrogen peroxide on oxygen-fed graphite/PTFE electrodes modified by 2-ethylanthraquinone. J. Electroanal. Chem. **601**, 63–67 (2007). doi:10.1016/j.jelechem.2006.10.023
7. F. Xu, T. Song, Y. Xu, Y. Chen, S. Zhu, S. Shen, A new cathode using CeO2/MWNT for hydrogen peroxide synthesis through a fuel cell. J. Rare Earths **27**, 128–133 (2009). doi:10.1016/S1002-0721(08)60206-9
8. S. Marcotte, D. Villers, N. Guillet, L. Roue, J.P. Dodelet, Electroreduction of oxygen on Co-based catalysts: determination of the parameters affecting the two-electron transfer reaction in an acid medium. Electrochim. Acta **50**, 179–188 (2004)
9. S. Damyanova, P. Grange, B. Delmon, Surface characterization of zirconia-coated alumina and silica carriers. J. Catal. **168**, 421–430 (1997). doi:10.1006/jcat.1997.1671
10. A. Moraes, M.H.M.T. Assumpção, F.C. Simões, V.S. Antonin, M.R.V. Lanza, P. Hammer, et al., Surface and catalytical effects on treated carbon materials for hydrogen peroxide electrogeneration. Electrocatalysis **7**, 60–69 (2016). doi:10.1007/s12678-015-0279-5
11. T. Mittermeier, P. Madkikar, X. Wang, H.A. Gasteiger, M. Piana, ZrO_2 based oxygen reduction catalysts for PEMFCs: towards a better understanding. J. Electrochem. Soc. **163**, F1543–F1552 (2016). doi:10.1149/2.0901614jes
12. Y. Liu, S. Akimitsu Ishihara, N. Mitsushima, K. Kamiya, Ota, transition metal oxides as DMFC cathodes without platinum. J. Electrochem. Soc. **154**, B664–B669 (2007)
13. T. Iwazaki, H. Yang, R. Obinata, W. Sugimoto, Y. Takasu, Oxygen-reduction activity of silk-derived carbons. J. Power Sources **195**, 5840–5847 (2010). doi:10.1016/j.jpowsour.2009.12.135
14. M.H.M.T. Assumpção, A. Moraes, R.F.B. De Souza, I. Gaubeur, R.T.S. Oliveira, V.S. Antonin, et al., Low content cerium oxide nanoparticles on carbon for hydrogen peroxide electrosynthesis. Appl. Catal. A Gen. **411–412**, 1–6 (2012). doi:10.1016/j.apcata.2011.09.030
15. M.H.M.T. Assumpção, R.F.B. De Souza, R.M. Reis, R.S. Rocha, J.R. Steter, P. Hammer, et al., Low tungsten content of nanostructured material supported on carbon for the degradation of phenol. Appl. Catal. B Environ. **142–143**, 479–486 (2013). doi:10.1016/j.apcatb.2013.05.024
16. M.P. Pechini, N. Adams, Method of preparating lead and alkaline earth titanates and niobates and coating method using the same to form a capacitor, US Pat. 3330697. (1967)
17. U.A. Paulus, T.J. Schmidt, H.A. Gasteiger, R.J. Behm, Oxygen reduction on a high-surface area Pt/Vulcan carbon catalyst: a thin-film rotating ring-disk electrode study. J. Electroanal. Chem. **495**, 134–145 (2001). doi:10.1016/S0022-0728(00)00407-1
18. J. Zhou, Y. Zu, A.J. Bard, Scanning electrochemical microscopy Part 39. The proton/hydrogen mediator system and its application to the study of the electrocatalysis of hydrogen oxidation. **491**, 22–29 (2000)
19. N. Diab, W. Schuhmann, Microelectrochemical visualization of oxygen consumption of single living cells. 19–32 (2013). doi:10.1039/c3fd00011g.
20. A. V. Naumkin, A. Kraut-Vass, S.W. Gaarenstroom, C.J. Powell, *NIST X-ray Photoelectron Spectroscopy Database. NIST Standard Database 20, Version 4.1*, http:/srdata.nist.gov/XPS/, (n.d.)
21. J.F. Carneiro, M.J. Paulo, M. Siaj, A.C. Tavares, M.R.V. Lanza, Nb2O5 nanoparticles supported on reduced graphene oxide sheets as electrocatalyst for the H2O2 electrogeneration. J. Catal. **332**, 51–61 (2015). doi:10.1016/j.jcat.2015.08.027
22. J.F. Carneiro, R.S. Rocha, P. Hammer, R. Bertazzoli, M.R.V. Lanza, Hydrogen peroxide electrogeneration in gas diffusion electrode nanostructured with Ta2O5. Appl. Catal. A Gen. **517**, 161–167 (2016). doi:10.1016/j.apcata.2016.03.013
23. R.B. Valim, R.M. Reis, P.S. Castro, A.S. Lima, R.S. Rocha, M. Bertotti, et al., Electrogeneration of hydrogen peroxide in gas diffusion electrodes modified with tert -butyl-anthraquinone on carbon black support, Carbon N. Y. **61**, 236–244 (2013). doi:10.1016/j.carbon.2013.04.100.
24. Y. Tan, C. Xu, G. Chen, X. Fang, N. Zheng, Q. Xie, Facile synthesis of manganese-oxide-containing mesoporous nitrogen-doped carbon for efficient oxygen reduction. Adv. Funct. Mater. **22**, 4584–4591 (2012)
25. A.J. Bard, L.R. Faulkner, *Electrochemical methods: fundamentals and applications* (New York, n.d.)
26. F. Wang, S. Hu, Studies of electrochemical reduction of dioxygen with RRDE. Electrochim. Acta **51**, 4228–4235 (2006)
27. Y. Liang, Y. Li, H. Wang, J. Zhou, J. Wang, T. Regier, et al., Co3O4 nanocrystals on graphene as a synergistic catalyst for oxygen reduction reaction. Nat. Mater. **10**, 780–786 (2011). doi:10.1038/nmat3087
28. L. Zhou, M. Zhou, Z. Hu, Z. Bi, K.G. Serrano, Chemically modified graphite felt as an efficient cathode in electro-Fenton for p-nitrophenol degradation. **140**, 376–383 (2014)